

# MEMBRANE INTERACTIONS IN NERVE MYELIN

## I. Determination of Surface Charge from Effects of pH and Ionic Strength on Period

HIDEYO INOUE AND DANIEL A. KIRSCHNER

*Department of Neuroscience, Children's Hospital, and Department of Neuropathology, Harvard Medical School, Boston, Massachusetts 02115*

**ABSTRACT** We have used x-ray diffraction to study the interactions between myelin membranes in the sciatic nerve (PNS) and optic nerve (CNS) as a function of pH (2–10) and ionic strength (0–0.18). The period of myelin was found to change in a systematic manner with pH and ionic strength. PNS periods ranged from 165 to 250 Å or more, while CNS periods ranged from 150 to 230 Å. The native periods were observed only near physiological ionic strength at neutral or alkaline pH. The smallest periods were observed in the pH range 2.5–4 for PNS myelin and pH 2.5–5 for CNS myelin. The minimum period was also observed for PNS myelin after prolonged incubation in distilled water. At pH 4, within these acidic pH ranges, myelin period increased slightly with ionic strength; however, above these ranges, the period increased with pH and decreased with ionic strength. Electron density profiles calculated at different pH and ionic strength showed that the major structural alteration underlying the changes in period was in the width of the aqueous space at the extracellular apposition of membranes; the width of the cytoplasmic space was virtually constant.

Assuming that the equilibrium myelin periods are determined by a balance of nonspecific forces/i.e., the electrostatic repulsion force and the van der Waals attractive force, as well as the short-range repulsion force (hydration force, or steric stabilization), then values in the period-dependency curve can be used to define the isoelectric pH and exclusion length of the membrane. The exclusion length, which is related to the minimum period at isoelectric pH, was used to calculate the electrostatic repulsion force given the other forces. The electrostatic repulsion was then used to calculate the surface potential, which in turn was used to calculate the surface charge density (at different pH and ionic strength). We found the negative surface charge increases with pH at constant ionic strength and with ionic strength at constant pH. We suggest that the former is due to deprotonation of the ionizable groups on the surface while the latter is due to ion binding. Interpretation of our data in terms of the chemical composition of myelin is given in the accompanying paper (Inouye and Kirschner, 1988). We also calculated the total potential energy functions for the different equilibrium periods and found that the energy minima became shallower and broader with increasing membrane separation. Finally, it was difficult to account directly for certain structural transitions from a balance of nonspecific forces. Such transitions included the abrupt appearance of the native period at alkaline pH and physiological ionic strength and the discontinuous compaction after prolonged treatment in distilled water. Possibly, in PNS myelin conformational modification of P0 glycoprotein occurs under these conditions. The invariance of the cytoplasmic space suggests the presence of specific short-range interactions between surfaces at this apposition.

### INTRODUCTION

Internodal myelin is the multilamellar, lipid-rich portion of the nerve myelin sheath that lies between the excitable nodes of Ranvier. This membrane assembly exhibits a regularity of membrane packing (Schmitt et al., 1935), and facilitates nerve conduction by providing a high resistance, low capacitance insulation around axons (Rushton, 1951; Tasaki, 1955; see also review by Ritchie, 1984). In

certain disease states where myelin organization is disrupted, nerve conduction falters (see review by Raine, 1984).

X-ray diffraction has been used to probe the interactions that stabilize the normal, orderly packing of myelin membranes by examining myelin structure in nerves which have been subjected to a variety of physical-chemical treatments. Such treatments involve changes in ionic strength (Finean and Millington, 1957; Robertson, 1958; Worthington and Blaurock, 1969), pH (Worthington, 1979), water content (Finean, 1961; Kirschner and Caspar, 1975), and temperature (Worthington and Worthington, 1981), and also exposure to chemical reagents (see reviews

Please address all correspondence to Dr. Daniel A. Kirschner, Department of Neuroscience, Children's Hospital, 300 Longwood Avenue, Boston, MA 02115

by Rumsby and Crang, 1977, and Kirschner et al., 1984). The changes in myelin period which result from these treatments have been summarized (Worthington, 1982; Kirschner et al., 1984), and the involvement of surface charge in determining membrane packing in myelin has been suggested (Worthington and Blaurock, 1969).

The equilibrium separation between membrane surfaces is largely determined by a balance of forces: van der Waals attraction and electrostatic repulsion (Verwey and Overbeek, 1948; Parsegian, 1973; Rand, 1981), the undulation force (Helfrich, 1977), and short-range repulsion due to hydration (Rand, 1981; Marčelja and Radić, 1976) or steric stabilization (Napper, 1977; Bell et al., 1984). The significance of the long-range forces of van der Waals attraction and electrostatic repulsion in macromolecular interaction has been recognized in the areas of colloid stability (Verwey and Overbeek, 1948), lipid bilayers (Rand, 1981), virus assembly (Bernal and Fankuchen, 1941; Millman et al., 1984), muscle fiber assembly (Rome, 1968; Elliot, 1968; Millman and Nickel, 1980), and biological membranes (Diederichs et al., 1985; Sculley et al., 1980). The van der Waals force, acting over hundreds of Angstroms, results from fluctuating electronic charges. The electrostatic force, also acting over large distances, results from an osmotic pressure that arises from the concentration gradient of diffusible ions at a membrane surface containing fixed charges. The undulation force, arising from the out-of-plane fluctuations of fluid membrane that are sterically hindered in multilayer systems, is thought to be the long-range repulsion force that counters van der Waals attraction (Helfrich, 1978; Evans and Parsegian, 1986). The short-range repulsion force, which has been proposed to account for the resistance to close-packing of apposed bilayers (reviewed by Rand, 1981) or membranes (Rand et al., 1979), may be due to surface hydration (Marčelja and Radić, 1976) and/or steric stabilization (Napper, 1977; Bell et al., 1984).

The surface charge density at neutral pH of myelin membranes was first evaluated by Rand et al. (1979) in frog peripheral nerve from measurement of the repulsive force acting between membranes. The observed decay of this force with membrane separation was shown to be similar to that for the electrostatic repulsion between model lipid bilayers. We have recently found that mouse sciatic nerve myelin swells in the range of pH 4–9 at reduced ionic strength (0.06), and also at ionic strengths <0.08 at constant pH 7 (Inouye et al., 1985). Such swelling is consistent with the expected increase in electrostatic repulsion when the negative surface charge increases with pH and when the counterion screening length increases in lowered salt. Here we have used x-ray diffraction to study more thoroughly the pH and ionic strength dependency of the widths of the inter-membrane spaces in sciatic nerve (PNS) myelin as well as in optic nerve (CNS) myelin, and have calculated the surface charge density of the membranes. In the accompanying paper (Inouye and

Kirschner, 1988), we have determined to what extent the known composition and localization of lipids and proteins in myelin are consistent with the observed myelin period and surface charge density. Preliminary reports of some of this work have been presented (Inouye and Kirschner, 1986a,b).

## MATERIALS AND METHODS

### Specimens

Sciatic nerves were dissected from adult normal (+ / +) and homozygous shiverer (*shi/shi*) mice and optic nerves were dissected from adult normal mice. The sciatic nerves were tied off at both ends, while the optic nerves were left untied. The nerves were incubated at room temperature in bulk test solutions for ~24 h. The pH was controlled by: HCl at pH 2; glycine and HCl at pH 2.1–3.6; formic acid and NaOH at pH 3.1–4.3; sodium acetate and acetic acid at pH 4.2–5.1; sodium mono- and di-basic phosphates at pH 6.1–8.1; Tris base and HCl at pH 7.6–8.9; and glycine and NaOH at pH 9.0–10.6. The overlapping pH ranges of the different buffer systems allowed for possible specific buffer effects. NaCl or KCl were used to maintain the pH solutions at constant ionic strength 0.06 or 0.15. Some nerves were treated in unbuffered media with the pH adjusted by HCl and NaOH. The reversibility of pH treatments was tested by incubating nerves in physiological saline at pH 7 after incubation at pH 2, 3, and 9 at constant ionic strength 0.06. For both PNS and CNS myelin, the structural modifications at pH 3 and 9 were reversible to the native state, whereas those at pH 2 were not. It is the reversible structural alterations such as these, which are considered in this paper. The effect of ionic strength in the range 0.01–0.20 was studied by adding NaCl to a particular buffer at constant pH 4, 5, 6, 7, and 9.7 (maximum deviation 0.2 pH). After incubation the nerves were sealed in thin-wall quartz capillaries containing test solution.

### X-ray Diffraction

Diffraction experiments were carried out using the nickel-filtered and single-mirror focused CuK $\alpha$  radiation from a fine-line source on an x-ray generator (Rigaku USA Inc., Danvers, MA) operated at 40 kV, 20 mA. The diffraction patterns were recorded during 1 h exposures with direct exposure x-ray film (Eastman Kodak Co., Rochester, N.Y.); for certain specimens longer exposures of ~20 h were taken to detect the higher order reflections. The specimen-to-film distance was 208 mm.

### Analysis of X-ray Diffraction Patterns

Myelin repeat periods were measured directly off the x-ray film using an optical densities of the films were determined on a Photoscan P-1000 microdensitometer (with a 25 or 50  $\mu$ m raster) (Optronics International, Inc., Chelmsford, MA) interfaced with a VAX 11/780 computer. The electron density profiles were calculated assuming that the modified structures closely resemble the native structure and that the packing of membranes across cytoplasmic and extracellular appositions were variable (Caspar and Kirschner, 1971; Kirschner and Ganser, 1982). To compare profiles, we measured the distance from polar headgroup peak across the cytoplasmic or extracellular gap to the corresponding peak in the neighboring bilayer.

## EXPERIMENTAL RESULTS

### pH-Dependency of Myelin Period

X-ray diffraction patterns of PNS and CNS myelin after treatments at constant ionic strength showed that the myelin periods varied systemically with pH (Figs., 1–2). In the diffraction patterns from the compact phase, the odd

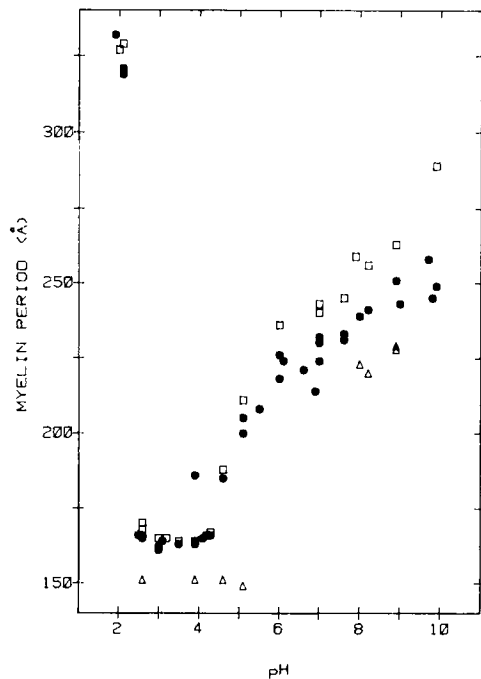


FIGURE 1 Myelin period in optic ( $\Delta$ ) and sciatic ( $\bullet$ , normal;  $\square$ , shiverer) nerves as a function of pH at a constant ionic strength of 0.06.

order reflections were weak, while in patterns from the swollen phase, the odd orders were as strong as the even orders (Inouye et al., 1985).

At an ionic strength of 0.06, PNS myelin swelled from its most compact period of  $\sim 165$  Å in the range of pH 2.5–4.5 to its maximum period of  $\sim 250$  Å at pH 9 (Fig. 1). Although the native period for mouse myelin is 178 Å, no periods intermediate to 165 Å and 185 Å were observed. As we have shown previously, the amount of swelling was always greater for shiverer myelin (Inouye et al., 1985). The native period for mouse myelin is 178 Å. Below pH 2 myelin swelled to the extreme value of  $\sim 330$  Å. At physiological ionic strength (0.15; Fig. 2), PNS myelin was at its most compact period of  $\sim 165$  Å at pH 3–4, but some nerves also showed a slightly swollen 185 Å-period phase in this pH range. At pH 4–7 more of the myelin was in the

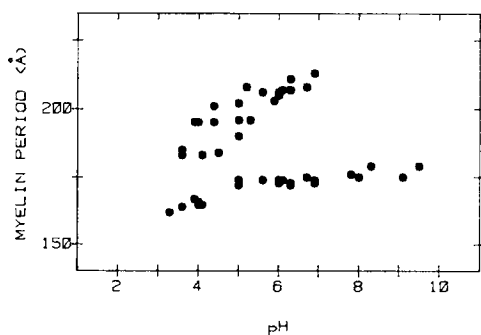


FIGURE 2 Myelin period in sciatic nerve as a function of pH at a constant ionic strength of 0.15.

swollen state and the period was 210 Å. At pH 5 the native period phase was first found to coexist with the swollen phase and the native phase became dominant with pH. Above pH 7 the myelin gradually swelled to 180 Å at pH 9.5. Similar patterns are observed after treatment with alkaline saline (Inouye and Kirschner, 1984). The diffraction patterns revealed no intermediate phases between the compact phase at  $\sim 165$  Å, the swollen phase at 185–210 Å, and the native-life phase at 172–180 Å (Fig. 2).

In the CNS at constant ionic strength 0.06, myelin had its most compact period of  $\sim 150$  Å in the range of pH 2.4–5.0 (Fig. 1). Between pH 5–8 the diffraction patterns were indistinct and multiple phase were recorded. At pH 8–9 a single 230 Å-swollen phase was observed.

### Ionic Strength Dependency of Myelin Period

The ionic strength-dependent interactions between myelin membranes were studied at pH 4, 5, 6, 7, and 9.7. At pH 7 and at an ionic strength of 0.12–0.14, a portion of PNS myelin swelled discontinuously from the native period to  $\sim 220$  Å (Fig. 3); the rest remained at the native period. As the ionic strength decreased from 0.14 to 0.10, a greater proportion of the myelin swelled. Below an ionic strength of 0.10 only the swollen phase was observed. As the ionic strength decreased further to 0.02, the myelin continued to swell to even large periods. At pH 4 over the range of ionic strengths 0.01–0.20, there was a slight increase in the PNS myelin period from 163 Å to 167 Å (Fig. 4). At pH 5, 6, and 9.7 the period of PNS myelin decreased as the ionic strength increased over the range studied (Fig. 5). At any particular ionic strength below  $\sim 0.10$ , periods were always greater at higher pH than at lower pH. At ionic strength 0.15 the myelin at pH 7 or 9.7 showed the native phase, while at pH 5 and 6 the myelin period was still 10–20 Å greater than the native. For the shiverer nerves, the dependence of myelin period on ionic strength was like that in normal nerves, but the periods were always greater than normal (Fig. 3; see also Inouye et al., 1985).

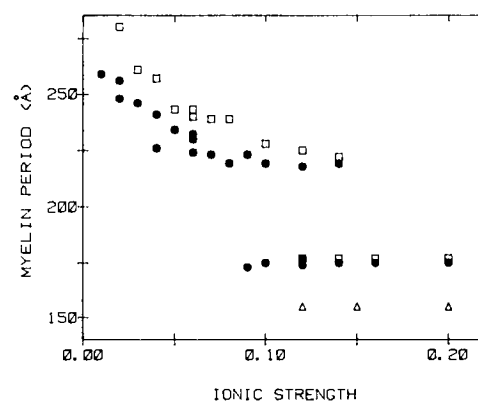


FIGURE 3 Myelin period in optic ( $\Delta$ ) and sciatic ( $\bullet$ , normal;  $\square$ , shiverer) nerves as a function of ionic strength at constant pH 7.

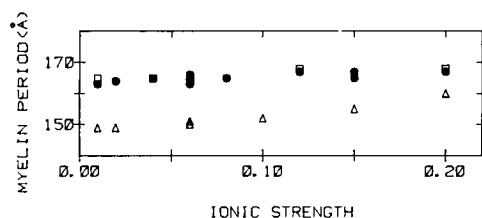


FIGURE 4 Myelin period in optic ( $\Delta$ ) and sciatic ( $\bullet$ , normal;  $\square$ , shiverer) nerves as a function of ionic strength at constant pH 4.

For CNS myelin incubated at constant pH 7, the native x-ray pattern was observed only at ionic strengths  $> 0.10$  (Fig. 3). At lower ionic strength the diffraction patterns were indistinct and showed multiple phases. When incubated at pH 4 CNS myelin swelled gradually from 147 Å at ionic strength 0.01 to 160 Å at ionic strength 0.20 (Fig. 4).

### Compaction of PNS Myelin in Distilled Water

Diffraction patterns from sciatic nerves were recorded after different incubation times in distilled water. As previously observed, the period increased for both normal and shiverer myelins and reached constant values of  $\sim 280$  Å and 340 Å, respectively, after  $\sim 20$  h (Inouye et al., 1985). Further incubation in distilled water resulted in a discontinuous compaction (Fig. 6). The  $\sim 165$  Å period and the diffracted intensity were similar to those obtained from PNS myelin incubated at pH 3–4 (Fig. 1; and see above). Shiverer myelin both swelled sooner and compacted sooner than did normal nerve myelin. Incubation of the compacted myelin in saline at neutral pH for  $\sim 24$  h restored the myelin to its native period, while incubation with 1 mM NaCl restored the swollen array. To determine whether the collagen that surrounds the myelinated fibers was involved in the compaction, some of the samples were pretreated with 0.1% collagenase in saline for 2 h (Rand et al., 1979),

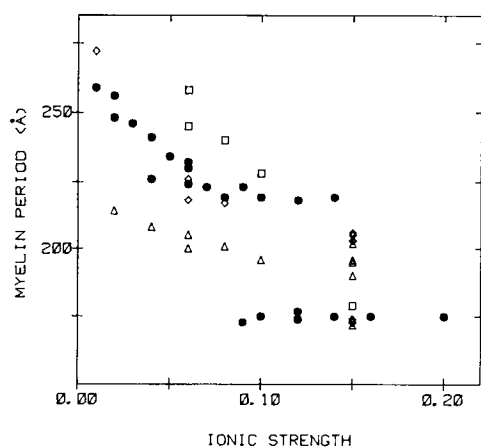


FIGURE 5 Myelin period in sciatic nerve as a function of ionic strength at constant pH 5 ( $\Delta$ ), 6 ( $\diamond$ ), 7 ( $\bullet$ ), and 9.7 ( $\square$ ).

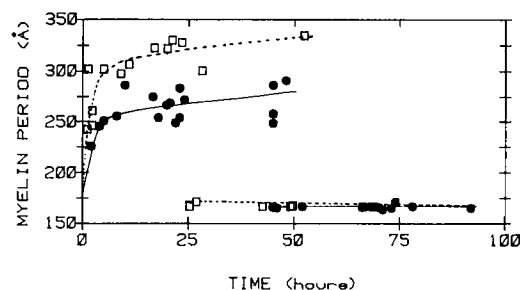


FIGURE 6 Swelling of normal ( $\bullet$ ) and shiverer ( $\square$ ) nerve myelins in distilled water. Ordinate, myelin period measured from x-ray diffraction patterns recorded for 1–4 h. Abscissa, treatment time for whole nerve in bulk distilled water. The curves were visually fit to the data points.

and then incubated in distilled water. Compaction to the 165 Å-period structure, as well as reversibility to the native-period structure, were still observed.

### Site of Swelling and Compaction in Myelin

Electron density profiles of myelin were calculated from the diffraction patterns at different pH. Comparison of the dimensions of the profiles, i.e., cytoplasmic space, bilayer thickness, and extracellular space (Table I) showed that changes in the membrane separation at the extracellular boundary accounted for most of the change in period. In PNS myelin, the extracellular space had a minimum width of 36 Å in the 165 Å-period compacted arrays, a native width of 49 Å, and a maximum width of over 100 Å in the swollen arrays. In CNS myelin, the minimum, native and maximum widths for the extracellular space were 30, 32, and 103 Å. In both types of myelin, the cytoplasmic space varied by only 1–2 Å from its native width of 33 Å in PNS myelin and 31 Å in the CNS. Thus, the interaction between extracellular surfaces of the membranes depended strongly on pH and ionic strength, while the interaction between the cytoplasmic surfaces was apparently indepen-

TABLE I  
MEASUREMENTS OF ELECTRON DENSITY PROFILES  
FROM MYELIN AT DIFFERENT pH AND IONIC  
STRENGTH

Sample	pH	$\mu$	d	2u	d-2u	cyt	lpg	ext
CNS	6.9	0.15	155	77	78	31	46	32
	4.6	0.06	150	75	75	30	45	30
	8.0	0.06	226	77	149	31	47	101
	8.9	0.06	229	78	151	32	47	103
PNS	7.3	0.16	178	80	98	33	48	49
	3.0	0.06	165	77	88	31	49	36
	8.1	0.06	234	81	153	34	48	104

$\mu$ , ionic strength; d, periodicity; 2u, center-to-center separation of the membranes at the cytoplasmic apposition; d-2u, center-to-center separation of the membranes at the extracellular apposition; cyt, cytoplasmic space; lpg, distance between lipid polar headgroups across the bilayer; ext, extracellular space. The dimensions (in Ångströms) were measured from profiles calculated from x-ray diffraction data to  $\sim 30$ – $40$  Å spacing (e.g., see inset of Fig. 7, and Inouye and Kirschner, 1984).

dent of the ionization state of these surfaces, except possibly under extreme conditions of low pH which results in irreversible transitions (Inouye et al., 1985).

## INTERPRETATION OF THE EXPERIMENTAL RESULTS

### Nonspecific Forces Acting Between the Membranes

Membrane packing and lattice stability in a multilamellar assembly such as myelin might be determined by interactions beyond nearest neighbors; however, for our analysis, we will only consider interactions between two apposed surfaces across an intervening electrolyte solution.

When the surfaces are charged the diffusable counterions that are of opposite charge tend to accumulate close to the surface. Given the potential at the midpoint between surfaces  $\phi(d_w/2)$ , where  $d_w$  is the separation between membranes, the electrolyte concentration is greater than

the bulk concentration, which causes an osmotic pressure and a repulsion force  $F_r$  per unit area (Fig. 7; Verwey and Overbeek, 1948)

$$F_r = 2nkT [\cosh[e\phi(d_w/2)/kT] - 1], \quad (1)$$

where  $n$  is the univalent electrolyte concentrations,  $e$  is the elementary charge,  $k$  is the Boltzmann constant, and  $T$  is the absolute temperature.

When the surface potential is small the potential at the midpoint between the pair of membranes is approximately equal to twice that at the same distance from the surface of an isolated membrane (Verwey and Overbeek, 1948). If the immersion medium consists of a univalent electrolyte of concentration  $n$ , the potential  $\phi(x)$  at position  $x$ , the surface potential  $\phi(x_s)$ , and the surface charge density  $\sigma$  are related as,

$$\tanh[Y(x)/4] = \tanh[Y(x_s)/4] \exp(-\kappa x) \quad (2)$$

$$\sigma = (\epsilon kT/2\pi e) \kappa \sinh(Y(x_s)/2), \quad (3)$$

where  $Y(x) = e\phi(x)/kT$  and  $\kappa$  is the Debye parameter equal to  $[8\pi e^2 n/(\epsilon kT)]^{1/2}$ .

The undulation force has recently been proposed as the long-range repulsion force that counters van der Waals attraction in lipid bilayer systems (Helfrich, 1978; Evans and Parsegian, 1986). The force per unit area is

$$F_{und} = 0.46(kT)^2/(k_c d_{eff}^3), \quad (4)$$

where  $k_c$  is the elastic modulus and  $d_{eff}$  is the effective separation between membranes. The exact front of the undulation force is not known. We assumed that  $d_{eff}$  is the same as  $d_w$  (see Eq. 1). Values for  $k_c$  have been determined for phosphatidylcholine bilayers and range from 1 to  $20 \times 10^{-13}$  erg (summarized by Beblin et al., 1985).

The short-range repulsion force (Eq. 5; Fig. 7), which was previously measured directly for myelin of frog sciatic nerve (Rand et al., 1979), dominates at membrane separations  $< 27 \text{ \AA}$ . This repulsion between membranes may arise from hydration (Marćelja and Radić, 1976), steric stabilization (Napper, 1977; Bell et al., 1984), or the undulation of the membranes (Sornette and Ostrowsky, 1986; Evans and Parsegian, 1986). We assumed the short-range repulsion force is expressed by the exponential form for the hydration force (LeNeveu et al., 1977).

$$F_h = K \exp(-d_w/L), \quad (5)$$

where  $L = 1.93 \text{ \AA}$ ,  $K = 1 \times 10^{11}$  for the force in units of dyn/cm<sup>2</sup>, and  $d_w$  is the separation between membranes (see Eq. 1).

Such repulsive forces (Eqs. 1, 4, and 5) are countered by the van der Waals attractive force (Verwey and Overbeek, 1948)

$$F_a = (H/6\pi) [1/d_w^3 - 2/(d_w + d_{ex})^3 + 1/(d_w + 2d_{ex})^3], \quad (6)$$

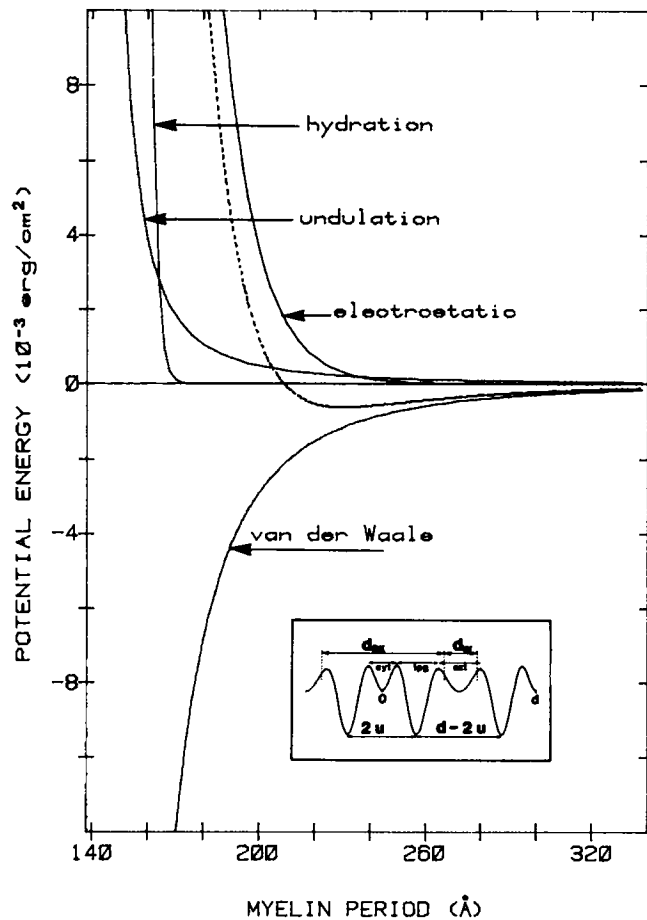


FIGURE 7 (a) Potential energy curves for the model of normal PNS myelin at pH 7 and ionic strength 0.06. The Hamaker coefficient was taken as  $5 \times 10^{-14}$  erg and the elastic modulus was  $2 \times 10^{-12}$  erg. The minimum in the net potential energy curve (dashes) gives the equilibrium period under these conditions. Inset, Schematic of electron density distribution calculated from the x-ray diffraction data showing the structural parameters listed in Table I and defined in Eq. (7).

where  $H$  is the Hamaker coefficient,  $d_{\text{ex}}$  is the distance from one charged extracellular surface across the membrane pair to the other extracellular surface (or exclusion length; see inset of Fig. 7), and the force is calculated per unit area.

For our calculation of the van der Waals attraction (Eq. 6, Fig. 7) we assigned the average value  $5.0 \times 10^{-14}$  erg to the Hamaker coefficient. Previous values for this coefficient obtained either by experiment or theoretical calculation range from 1 to  $10 \times 10^{-14}$  erg. These values were determined for a number of diverse systems: hydrocarbon (Gingell and Parsegian, 1972; Haydon and Taylor, 1968), lipid bilayers having different protein and sugar coats or polar headgroups (Nir and Anderson, 1977; Brooks et al. 1975), thylakoid membranes (Sculley et al., 1980), phosphatidylcholine bilayers (Requena and Haydon, 1975; Parsegian et al., 1979; Evans and Metcalfe, 1984; Marra, 1986; Ohshima et al., 1982; Lis et al., 1982), phosphatidylserine bilayers (Loosley-Millman et al., 1982), and phosphatidylethanolamine bilayers (Lis et al., 1982; Marra, 1986). In addition, the Hamaker coefficient apparently decreases in the presence of salt (Marra, 1986).

The net force ( $F_{\text{net}}$ ) between the apposed membranes, given by the summation of the forces ( $F_r + F_h + F_{\text{und}} - F_a$ ), is zero at the equilibrium period. Integration of the individual forces (Eqs. 1, 4, 5, and 6) gives the potential energy functions  $V_r$ ,  $V_h$ ,  $V_{\text{und}}$  and  $V_a$  (Fig. 7). At the equilibrium separation the net potential energy ( $V_{\text{net}} = V_r + V_h + V_{\text{und}} - V_a$ ) is a minimum and less than zero. In such a calculation the mechanical constraints due to collagen surrounding the individual myelinated nerve fibers (in the PNS) need not be included because collagen does not apparently restrict the swelling at membrane separations below the swelling limit (Rand et al., 1979; see also Inouye et al., 1985).

The myelin period  $d$  is related to the inter-membrane separation  $d_w$  by:

$$d = d_w + d_{\text{ex}}. \quad (7)$$

We assumed that the charge is restricted to a smooth surface.  $d_w$  consists of the tightly bound hydration water plus the readily exchangeable water. At closest approach (i.e., in the isoelectric pH range; see below), the myelin period is equal to the exclusion length plus the thickness of the hydration layer.

We obtained a first approximation of the exclusion length as follows. The most compact periods of myelin, obtained at pH  $\sim 4$  (see Figs. 1 and 2), were  $\sim 165$  Å for PNS myelin and  $\sim 150$  Å for CNS myelin. At the isoelectric pH the charge density is effectively zero, so the myelin period results from a balance between the strong hydration repulsion and the van der Waals attraction. Using a Hamaker coefficient of  $5.0 \times 10^{-14}$  erg for the van der Waals attraction, the balance was achieved when  $d_w$  is  $\sim 27$  Å. The exclusion lengths  $d_{\text{ex}}$  are then  $138$  Å ( $= 165 - 27$

Å) for PNS myelin and  $123$  Å ( $= 150 - 27$  Å) for CNS myelin. Since the distance between polar headgroup layers at the extracellular surfaces across the cytoplasmic boundary of a membrane pair is  $129$  Å for PNS and  $123$  Å for CNS myelin (Fig. 7, inset; Table I), then the surface charge front is located  $\sim 5$  Å away from the polar headgroup layer for PNS myelin but at the position of the headgroup layer for CNS myelin.

### Estimation of the Surface Charge Density

Knowing the exclusion length (which is constant) and the myelin period (which depends on pH and ionic strength) gave  $d_w$  (Eq. 7). Using  $d_w$ , we calculated  $F_{\text{und}}$ ,  $F_h$ , and  $F_a$  from Eqs. 4–6. At equilibrium,  $F_r$  was calculated from a balance of these forces. The electrostatic potential at the midpoint between the pair of membranes was evaluated from  $F_r$  using Eq. 1. From Eqs. 2 and 3 we calculated the potential at the surface (Eq. 2) and the charge density at the extracellular surfaces (Eq. 3) as a function of pH (Fig. 8) and ionic strength (Fig. 9).

The negative surface charges density increased with pH above its isoelectric point. The pI for CNS myelin appeared more alkaline than that for PNS myelin. Above the isoelectric point (at an ionic strength 0.06; Fig. 8 a), PNS myelin in the shiverer mutant was more negatively charged than the normal. The estimated surface charge density of PNS myelin at higher ionic strength (0.15; Fig. 8 b) was greater than that at lower ionic strength (0.06) above the isoelectric point. At this higher ionic strength and above pH 7, we also calculated a constant, slightly negative surface charge density which corresponds to the native-like period structure that coexists with the swollen arrays (see Fig. 2). At pH 5, 6, 7, and 9.7, the calculated negative surface charge density increased with ionic strength (Fig. 9).

The values taken for the Hamaker coefficient (Eq. 6) affected the calculated charge density. Using smaller values for the coefficient gave lower surface charge densities (insets of Figs. 8 a and 9). When the undulation force was included, with  $k_c = 2 \times 10^{-12}$  erg (Eq. 4), the surface charge density was slightly lower compared with its value in the absence of this force.

### Total Potential Energy of Membrane Packing

The total potential energy as a function of pH (at constant ionic strength 0.06) was calculated given the observed myelin periods from Fig. 1 and assuming a constant surface charge. As the pH increases the energy minimum becomes shallower and broader (Fig. 10). At  $\sim$ pH 4.6, two equilibrium periods at  $\sim 165$  Å and  $\sim 185$  Å are indicated by the double energy minima. The minimum giving the  $165$  Å period comes from a balance between the hydration and van der Waals forces, while that at  $185$  Å comes from a balance between the electrostatic and van der Waals

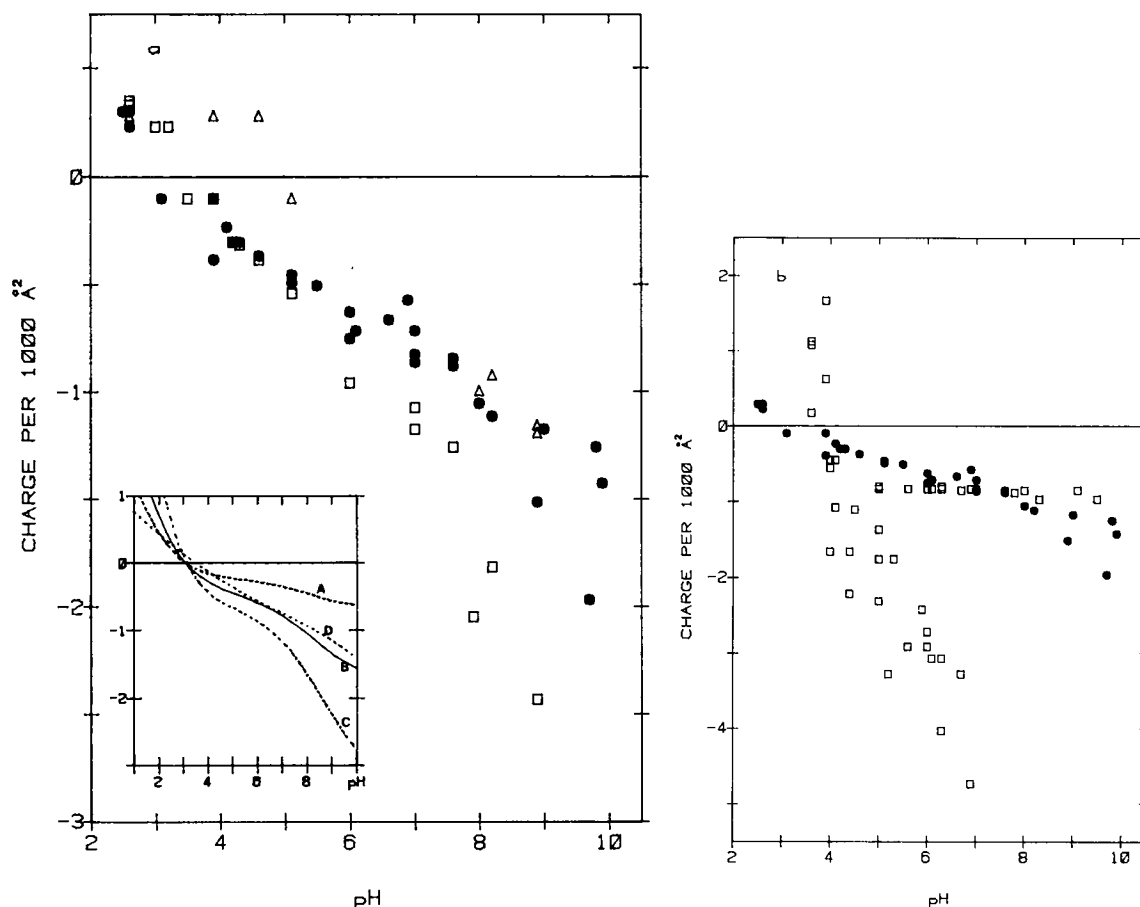


FIGURE 8 (a) Calculated surface charge densities for the extracellular surface of normal sciatic nerve (●), shiverer sciatic nerve (□), and normal optic nerve (Δ) as a function of pH at constant ionic strength. The ionic strength is 0.06, and the Hamaker coefficient is  $5 \times 10^{-14}$  erg with undulation force not included. *Inset*, Surface charge density calculated with different values of the Hamaker coefficient: A,  $1 \times 10^{-14}$  erg; B,  $5 \times 10^{-14}$  erg; C,  $10 \times 10^{-14}$  erg; or D, calculated with undulation force (for  $k_c = 2 \times 10^{-12}$  erg) and a Hamaker coefficient of  $5 \times 10^{-14}$  erg. (b) Calculated surface charge densities for normal sciatic nerve at ionic strength 0.15 (□) and at 0.06 (●). The Hamaker coefficient is  $5 \times 10^{-14}$  erg (with undulation force not included).

forces. This particular balance of forces apparently results in an absence of observed, intermediate periods between 165 Å and 185 Å (Fig. 1). Similar arguments explain the observed coexistence of two phases at ~pH 4.5 in physiological saline (ionic strength 0.15; Fig. 2).

## DISCUSSION

Membrane surface charge density is determined by the pK's of the ionizable groups in the surface, and the pH and ionic strength of the bathing medium (Ninham and Parsegian, 1971). By changing the proton and counterion concentrations, the electrostatic repulsion between the apposed membranes is altered, and the widths of the intermembrane spaces and the myelin period can be varied in a systematic manner (Inouye et al., 1985). Since protons are highly permeable across lipid bilayers and biological membranes (Gutknecht, 1984; Deamer and Bramhall, 1986), then changes in membrane separation could occur at both cytoplasmic and extracellular appositions. However, electron density profiles calculated from our x-ray

diffraction patterns of mouse nerves at different pH and ionic strength showed that the major structural alteration was in the width of the space at the extracellular apposition. Assuming that the space of this apposition is determined by nonspecific forces (as described above), we defined the isoelectric pH and exclusion length, and then estimated the pH titration curve of the surface charge density and the total potential energy between surfaces.

## Comparison with Previous Findings

### *Exclusion Lengths in CNS and PNS Myelin.*

Under isoelectric conditions where membranes exhibit their closest approach, the period of CNS myelin is 15 Å less than that of PNS myelin. Since the widths of the cytoplasmic space and membrane bilayer are similar in CNS and PNS myelins under these conditions, then the difference in period must arise from a greater projection of P0-glycoprotein (which is the integral membrane protein of PNS myelin) into the extracellular space compared with the projection of proteolipid protein (PLP, the integral

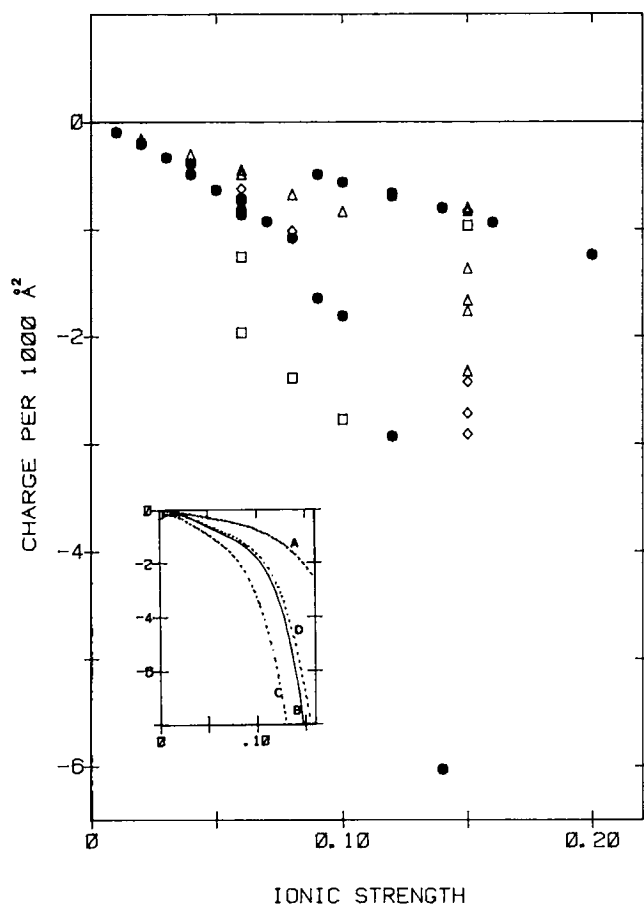


FIGURE 9 Calculated surface charge density for the extracellular surface of sciatic nerve as a function of ionic strength at constant pH 5 ( $\Delta$ ), 6 ( $\diamond$ ), 7 ( $\bullet$ ), and 9.7 ( $\square$ ). The Hamaker coefficient is  $5 \times 10^{-14}$  erg, and the undulation force is not included. Inset, Calculated surface charge density for the expanded phase (polynomial fit to the data points) as a function of ionic strength at pH 7 with different Hamaker coefficients: A,  $1 \times 10^{-14}$  erg; B,  $5 \times 10^{-14}$  erg; C,  $10 \times 10^{-14}$  erg; or D, calculated with undulation force ( $k_c = 2 \times 10^{-12}$  erg) and a Hamaker coefficient of  $5 \times 10^{-14}$  erg.

membrane protein of CNS myelin). This conclusion is consistent with previous x-ray diffraction and freeze-fracture studies (reviewed by Kirschner et al., 1984) and also with the postulated conformations of PLP and P0 which show a smaller extracellular domain in PLP (Stoffel et al., 1985) than in P0 (Lemke and Axel, 1985).

**Isoelectric pH.** The isoelectric ranges that we have measured and calculated for myelin are consistent with previous reports. Leitch et al. (1969) measured for CNS myelin isolated from bovine optic nerve the ratio of wet weight to dry weight after treatment in media at different pH. The minimum water content was observed at pH 4 and a rapid increase in water content was found at pH  $> 8$ . This correlates well with our observation and calculation of the closest approach of membranes (i.e., smallest period and minimum extracellular space) at pH  $\sim 4$ , and of the regular swelling of the membrane arrays at

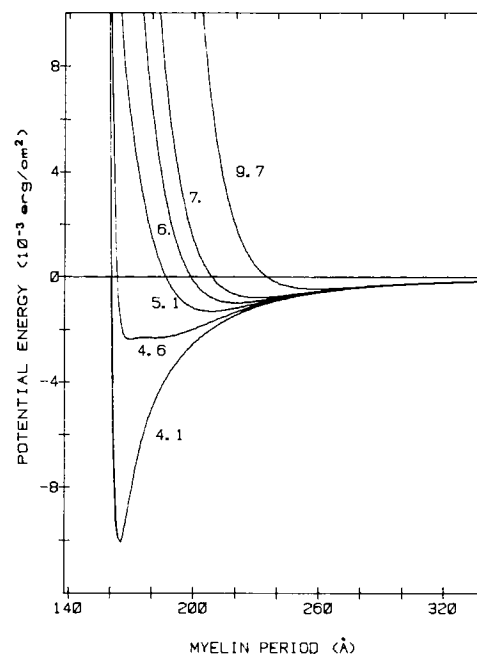


FIGURE 10 Net potential energy curves from the observed myelin period at constant ionic strength 0.06 and different pH (as indicated along the curves). The Hamaker coefficient is  $5 \times 10^{-14}$  erg, the undulation force. Note that the calculated double minimum at pH 4.6 corresponds to a discontinuous transition between membrane arrays having periods 165 and 185 Å, in agreement with the observations in Fig. 1.

pH 8–9 (Fig. 1). Feinstein and Felsenfeld (1975) studied the binding of anionic fluorescent probes to isolated myelin from bovine white matter and found that there was a drastic decrease in binding above pH 4, which suggests that this is the isoelectric point. Our finding that CNS myelin has a slightly more alkaline pI range than PNS myelin is consistent with previous results that CNS myelin can become compacted in distilled water (at  $\sim$ pH 5) (Kirschner and Sapirstein, 1982), whereas PNS myelin swells (Finean and Millington, 1957; Robertson, 1958).

**Surface Charge Density.** Our calculated values of charge (or potential) at the extracellular surface are in the range of values determined in other studies under conditions of very low ionic strength. From direct measurement of the electrostatic repulsion between membranes, Rand et al. (1979) reported a surface charge density of  $-2.0$  to  $-6.7 \times 10^{-4}/\text{\AA}^2$  for PNS myelin in frog sciatic nerve treated at pH 6.8 (0.001 M phosphate or Tris buffer). Our measurement of the surface charge for mouse sciatic nerve at pH 7 are in the range of  $-1$  to  $-10 \times 10^{-4}/\text{\AA}^2$  when the ionic strength is in the range of 0.01–0.08.

Moscarello et al. (1985) measured a zeta-potential of  $-66.6$  mV at pH 8.1 for CNS myelin isolated from normal human brain. From an apparent dissociation constant of 6 mM for calcium in bovine brain white matter at pH 7.4 (Feinstein and Felsenfeld, 1975) and an intrinsic dissocia-

tion constant of 50 mM for calcium from lipid polar groups (Ohshima et al., 1982), we calculated the surface potential in CNS myelin to be  $-26$  mV. How do these surface potentials compare with those from our data? If the surface charge density calculated from the myelin period at pH 8 and ionic strength 0.06 is constant at other ionic strengths, then the estimated surface potential is  $-86$  mV at ionic strength 3 mM (corresponding to the conditions of Moscarello et al., 1985) or  $-61$  mV at ionic strength 9 mM (corresponding to the conditions of Feinstein and Felsenfeld, 1975). The surface potentials from our data on CNS myelin are greater than the corresponding reported values. This may be due largely to charge reduction when the ionic strength decreases.

### Interpretation of Surface Charge-Dependence on pH and Ionic Strength

Our results show that the negative surface charge density at the extracellular surfaces of myelin increases with pH or ionic strength (Figs. 8 and 9). The pH-dependence, which is expected, can be accounted for by deprotonation of the ionizable groups when the pH increases. The ionic strength-dependence of the surface charge, which is surprising if one assumes that the mobile counterions screen the fixed charges, might be accounted for by three factors: (a) a shift of the proton dissociation constant of the ionizable groups on the surface; (b) a change in the Hamaker coefficient with ionic strength; and (c) binding of ions to the surface groups. When the surface potential is negative and the ionic strength is reduced, the proton dissociation constant should increase and the negative surface charge density become less. Given the localization of chemical components in the membrane surface, one can calculate the surface charge as a function of ionic strength; however, we have found that such a chemical model does not account for the large change in surface charge with ionic strength (see accompanying paper, Inouye and Kirschner, 1988). An increase in the Hamaker coefficient with ionic strength might also account for the observed dependency of surface charge on ionic strength; however, Marra (1986) has found that the coefficient actually decreases with ionic strength. The binding of cations and anions to the ionizable groups also could modify the surface charge (see accompanying paper, Inouye and Kirschner, 1988).

Similar disparities in comparing the calculated and observed ionic strength-dependency of charge have been reported in other organized macromolecular systems, e.g., in tobacco mosaic virus (Millman et al., 1984) and in muscle (Naylor et al., 1985). Larger values of calculated versus measured periods were explained variously in these papers by an entropy effect, by an inaccurate approximation using Poisson-Boltzmann statistics of the diffusible ion concentration, or by anion binding.

### Interpretation of Ionic Strength-Dependence of Period at Isoelectric pH

At pH 4, which is in the isoelectric range, the myelin period increased slightly with ionic strength. This small change in membrane separation may be accounted for by a reduction of the van der Waals attraction upon addition of electrolytes (Marra, 1986). By equating the van der Waals attraction force and the hydration force, we were able to calculate the Hamaker coefficient for myelin as a function of ionic strength. We found the coefficient decreased moderately from  $7 \times 10^{-14}$  erg to  $1 \times 10^{-14}$  erg when the ionic strength increased from 0.01 to 0.20. These values are consistent with the range of the Hamaker coefficient as previously reported (see text after Eq. 6).

### Surface Charge Density in Shiverer Myelin

Homozygous shiverer mice lack a major portion of the gene for myelin basic protein (Roach et al., 1983; Kimura et al., 1985), show a striking deficit of this protein in their dysmyelinated CNS and myelinated PNS (Dupouey et al., 1979; Kirschner and Ganser, 1980; Mikoshiba et al., 1981), and have an abnormal lipid composition in their PNS myelin (Inouye et al., 1985). In addition, certain inter-membrane interactions at the extracellular apposition are different in shiverer compared with normal PNS myelin (Inouye and Kirschner, 1984; Inouye et al., 1985). We previously calculated that the 20–25% increase of sulfatides (with a  $pK \sim 1.9$ ) in shiverer would correspond to a 10% increase in its surface charge, yet our interpretation of the x-ray measurements suggested a 70% increase in surface charge (Inouye et al., 1985). In that study, we had assumed that attractive forces were constant as a function of myelin period since the periods were linear with (ionic strength) $^{-1/2}$ . Here, however, we more correctly base our calculations on a balance of van der Waals attractive and electrostatic and hydration repulsive forces. We now calculate a 30% increase in the surface charge density in shiverer compared with normal (from Fig. 8a at pH 7 and ionic strength 0.06). This value, which is closer to, but still higher than that estimated before from the biochemical data, suggests that there are more ionizable groups in the extracellular surface of shiverer than in normal PNS myelin, possibly due to changes in the charge, conformation, or disposition of P0 glycoprotein (Inouye et al., 1985).

### Specific, Short-Range Interactions at the Extracellular Surface

Several occurrences of discontinuous structural transitions or coexisting phases were observed in our experiments. As explained above, nonspecific interactions defined by the attractive and repulsive forces can account for two such instances in PNS myelin at pH 4–5: the  $165 \text{ \AA} \rightarrow 185 \text{ \AA}$  period jump at ionic strength 0.06, and the two phases at

ionic strength 0.15. Other types of interactions must be invoked to explain the remaining examples. In PNS myelin, the 165 Å → 330 Å transition at pH 2 and ionic strength 0.06 was irreversible to the native structure. The 175 Å → 220 Å transition at pH 7 and ionic strength 0.08, and the ~220 Å → 178 Å transition at pH > 7 and ionic strength 0.15 were not predicted when it was assumed that the surface charge density is screened by electrolytes and is constant for different ionic strength. The ~300 Å → 165 Å compaction after prolonged treatment in distilled water appeared to be contrary to the increase of the screening length with decreasing ionic strength (see also accompanying paper, Inouye and Kirschner, 1988). Also, multiple phases were observed in CNS myelin at pH 4–8 and ionic strength 0.06. Types of specific, short-range forces that could underlie some of these intermembrane interactions that cannot be explained by nonspecific forces include, in order of increasing strength of interaction: electrostatic (salt-bridge or ion pair), hydrogen bond, and hydrophobic (Schulz and Schirmer, 1979).

## CONCLUSIONS

Our study demonstrates that the myelin period and particularly the width of the extracellular space are very sensitive to changes in pH and ionic strength, presumably due to charges on the apposed membrane surfaces. Since surface charge depends on the numbers and kinds of ionizable groups present (see accompanying paper, Inouye and Kirschner, 1988), then the use of "electrostatic stressing" may be generally applicable for detecting differences in inter-membrane interactions between myelins that appear to have similar "native" structures under physiological conditions. Such altered interactions may reveal compositional differences (Inouye et al., 1985), and may also herald functional differences. Conversely, the technique also provides a way of examining the possible consequences of demonstrated chemical differences.

We thank Dr. M.K. Wolf (Department of Anatomy, University of Massachusetts Medical School, Worcester, MA) for providing some of the shiverer and control mice used in these studies.

We are grateful to Drs. V. Adrian Parsegian and Barry M. Millman for invaluable comments on the manuscript.

The research was supported by National Institutes of Health grants NS-20824 (to Dr. Kirschner) and NS-11237 (to Dr. R.L. Sidman) from the National Institute of Neurological and Communicative Disorders and Stroke. The work was carried out in facilities of the Mental Retardation Research Center which is supported by National Institutes of Health core grant HD-06276.

Received for publication 27 May 1987 and in final form 25 September 1987.

## REFERENCES

Beblik, G., R.-M. Servuss, and W. Helfrich. 1985. Bilayer bending rigidity of some synthetic lecithins. *J. Physique*. 46:1773–1778.

- Bell, G. I., M. Dembo, and P. Bongrand. 1984. Cell adhesion: competition between nonspecific repulsion and specific bonding. *Biophys. J.* 45:1051–1064.
- Bernal, J. D., and I. Fankuchen. 1941. X-ray and crystallographic studies of plant virus preparations. *J. Gen. Physiol.* 25:111–165.
- Brooks, D. E., Y. K. Levine, J. Requena, and D. A. Haydon. 1975. Van der Waals forces in oil-water systems from the study of thin lipid films: III. Comparison of experimental results with Hamaker coefficients calculated from Lifshitz theory. *Proc. R. Soc. Lond. A Math. Phys. Sci.* 347:179–194.
- Caspar, D. L. D., and D. A. Kirschner. 1971. Myelin membrane structure at 10 Å resolution. *Nature (Lond.)*. 231:46–52.
- Deamer, D. W., and J. Bramhall. 1986. Permeability of lipid bilayers to water and ionic solutes. *Chem. Phys. Lipids*. 40:167–188.
- Diederichs, K., W. Welte, and W. Kreutz. 1985. Determination of interaction forces between higher plant thylakoids and electron-density-profile evaluation using small-angle x-ray scattering. *Biochim. Biophys. Acta*. 809:107–116.
- Dupouey, P., C. Jacque, J.-M. Bourre, F. Cesselin, A. Privat, and N. Baumann. 1979. Immunochemical studies of myelin basic protein in shiverer mouse devoid of major dense line of myelin. *Neurosci. Lett.* 12:113–118.
- Elliott, G. F. 1968. Force-balances and stability in hexagonally-packed poly-electrolyte systems. *J. Theor. Biol.* 21:71–87.
- Evans, E., and M. Metcalfe. 1984. Free energy potential for aggregation of giant, neutral lipid bilayer vesicles by van der Waals attraction. *Biophys. J.* 46:423–426.
- Evans, E. A., and V. A. Parsegian. 1986. Thermal-mechanical fluctuations enhance repulsion between bimolecular layers. *Proc. Natl. Acad. Sci. USA*. 83:7132–7136.
- Feinstein, M. B., and H. Felsenfeld. 1975. Reactions of fluorescent probes with normal and chemically-modified myelin. *Biochemistry*. 14:3041–3048.
- Finean, J. B. 1961. The nature and stability of nerve myelin. *Int. Rev. Cytol.* 12:303–336.
- Finean, J. B., and P. F. Millington. 1957. Effects of ionic strength of immersion medium on the structure of peripheral nerve myelin. *J. Biophys. Biochem. Cytol.* 3:89–94.
- Gingell, D., and V. A. Parsegian. 1972. Computation of van der Waals interactions in aqueous systems using reflectivity data. *J. Theor. Biol.* 36:41–52.
- Gutknecht, J. 1984. Proton/hydroxide conductance through lipid bilayer membranes. *J. Membr. Biol.* 82:105–112.
- Haydon, D. A., and J. L. Taylor. 1968. Contact angles for thin lipid films and the determination of London-van der Waals forces. *Nature (Lond.)*. 217:739–740.
- Helfrich, W. 1978. Steric interaction of fluid membranes in multilayer systems. *Z. Naturforsch.* 33a:305–315.
- Inouye, H., and D. A. Kirschner. 1984. Effects of ZnCl<sub>2</sub> on membrane interactions in myelin of normal and shiverer mice. *Biochim. Biophys. Acta*. 776:197–208.
- Inouye, H., and D. A. Kirschner. 1986a. Myelin membrane structure modeled to account for pH titration curves. *Trans. Am. Soc. Neurochem.* 17:156.
- Inouye, H., and D. A. Kirschner. 1986b. Modeling the extracellular and cytoplasmic surfaces of myelin from x-ray diffraction studies of membrane interactions. *Amer. Cryst. Assn. Annu. Mtg.* 14:44.
- Inouye, H., and D. A. Kirschner. 1988. Membrane interactions in nerve myelin: II. Determination of surface charge from biochemical data. *Biophys. J.* 53.
- Inouye, H., A. L. Ganser, and D. A. Kirschner. 1985. Shiverer and normal peripheral myelin compared: basic protein localization, membrane interactions and lipid composition. *J. Neurochem.* 45:1911–1922.
- Kimura, M., H. Inoko, M. Katsuki, A. Ando, T. Sato, T. Hirose, H. Takashima, S. Inayama, H. Okano, K. Takamatsu, K. Mikoshiba, Y. Tsukada, and I. Wantanabe. 1985. Molecular genetic analysis of

- myelin-deficient mice: shiverer mutant mice show deletion of gene(s) coding for myelin basic protein. *J. Neurochem.* 44:692–696.
- Kirschner, D. A., and D. L. D. Caspar. 1975. Myelin structure transformed by dimethylsulfoxide. *Proc. Natl. Acad. Sci. USA* 72:3513–3517.
- Kirschner, D. A., and A. L. Ganser. 1980. Compact myelin exists in the absence of basic protein in the shiverer mutant mouse. *Nature (Lond.)* 283:207–210.
- Kirschner, D. A., and A. L. Ganser. 1982. Myelin labeled with mercuric chloride: Asymmetric localization of phosphatidylethanolamine plasmalogen. *J. Mol. Biol.* 157:635–658.
- Kirschner, D. A., A. L. Ganser, and D. L. D. Caspar. 1984. Diffraction studies of molecular organization and membrane interactions in myelin. In *Myelin*. Morell, P., editor. pp 51–95, Plenum Publishing Co., New York.
- Kirschner, D. A., and V. S. Sapirstein. 1982. Triethyl tin-induced myelin oedema: an intermediate swelling state detected by x-ray diffraction. *J. Neurocytol.* 11:559–569.
- Laursen, R. A., M. Samiullah, and M. B. Lees. 1984. The structure of bovine brain proteolipid and its organization in myelin. *Proc. Natl. Acad. Sci. USA* 81:2912–2916.
- Leitch, G. J., L. A. Horrocks, and T. Samorajski. 1969. Effects of cations on isolated bovine optic nerve myelin. *J. Neurochem.* 16:1347–1354.
- LeNeveu, D. M., R. P. Rand, V. A. Parsegian, and D. Gingell. 1977. Measurement and modification of forces between lecithin bilayers. *Biophys. J.* 18:209–230.
- Lemke, G., and R. Axel. 1985. Isolation and sequence of a cDNA encoding the major structural protein of peripheral myelin. *Cell* 40:501–508.
- Lis, L. J., M. McAlister, N. Fuller, R. P. Rand, and V. A. Parsegian. 1982. Interactions between neutral phospholipid and bilayer membranes. *Biophys. J.* 37:657–665.
- Loosley-Millman, M. E., R. P. Rand, and V. A. Parsegian. 1982. Effects of monovalent ion binding and screening on measured electrostatic forces between charged phospholipid bilayers. *Biophys. J.* 40:221–232.
- Marćelja, S., and N. Radić. 1976. Repulsion of interfaces due to boundary water. *Chem. Phys. Lett.* 42:129–130.
- Marra, J. 1986. Direct measurements of attractive van der Waals and adhesion forces between uncharged lipid bilayers in aqueous solutions. *J. Colloid Interface Sci.* 109:11–20.
- Mikoshiba, K., S. Kohsaka, K. Takamatsu, and Y. Tsukada. 1981. Neurochemical and morphological studies on the myelin of peripheral nervous system from shiverer mutant mice: absence of basic proteins common to central nervous system. *Brain Res.* 204:455–460.
- Miller, A., and J. Woodhead-Galloway. 1971. Long range forces in muscle. *Nature (Lond.)* 229:470–473.
- Millman, B. M., and B. G. Nickel. 1980. Electrostatic forces in muscle and cylindrical gel systems. *Biophys. J.* 32:49–63.
- Millman, B. M., T. C. Irving, B. G. Nickel, and M. E. Loosley-Millman. 1984. Interrod forces in aqueous gels of tobacco mosaic virus. *Biophys. J.* 45:551–556.
- Moscarello, M. A., L.-S. Chia, D. Leighton, and D. Absalom. 1985. Size and surface charge properties of myelin vesicles from normal and diseased (multiple sclerosis) brain. *J. Neurochem.* 45:415–421.
- Napper, D. H. 1977. Steric stabilization. *J. Colloid Interface Sci.* 58:390–407.
- Naylor, G. R. S., E. M. Bartels, T. D. Bridgman, and G. F. Elliott. 1985. Donnan potentials in rabbit psoas muscle in rigor. *Biophys. J.* 48:47–59.
- Ninham, B. W., and V. A. Parsegian. 1971. Electrostatic potential between surfaces bearing ionizable groups in ionic equilibrium with physiologic saline solution. *J. Theor. Biol.* 31:405–428.
- Nir, S., and M. Anderson. 1977. Van der Waals interactions between cell surfaces. *J. Membrane Biol.* 31:1–18.
- Ohshima, H., Y. Inoko, and T. Mitsui. 1982. Hamaker constant and binding constants of  $\text{Ca}^{2+}$  and  $\text{Mg}^{2+}$  in dipalmitoyl phosphatidylcholine/water system. *J. Colloid Interface Sci.* 86:57–72.
- Parsegian, V. A. 1973. Long-range physical forces in the biological milieu. *Annu. Rev. Biophys. Bioeng.* 2:222–255.
- Parsegian, V. A., N. Fuller, and R. P. Rand. 1979. Measured work of deformation and repulsion of lecithin bilayers. *Proc. Natl. Acad. Sci. USA* 76:2750–2754.
- Raine, C. S. 1984. The neuropathology of myelin diseases. In *Myelin*. Morell, P., editor. pp. 259–310. Plenum Publishing Co., New York.
- Rand, R. P. 1981. Interacting phospholipid bilayers: measured forces and induced structural changes. *Annu. Rev. Biophys. Bioeng.* 10:277–314.
- Rand, R. P., N. L. Fuller, and L. J. Lis. 1979. Myelin swelling and measurement of forces between myelin membranes. *Nature (Lond.)* 279:258–260.
- Requena, J., and D. A. Haydon. 1975. Van der Waals forces in oil-water systems from the study of thin lipid films: II. The dependence of the van der Waals free energy of thinning on film composition and structure. *Proc. R. Soc. Lond. A Math. Phys. Sci.* 347:161–177.
- Ritchie, J. M. 1984. Physiological basis of conduction in myelinated nerve fibers. In *Myelin*. Morell, P., editor. pp. 117–145. Plenum Publishing Co., New York.
- Roach, A., K. Boylan, S. Horvath, S. B. Prusiner, and L. E. Hood. 1983. Characterization of cloned cDNA representing rat myelin basic protein: absence of expression in brain of shiverer mutant mice. *Cell* 34:799–806.
- Robertson, J. D. 1958. Structural alterations in nerve fibers produced by hypotonic and hypertonic solutions. *J. Biophys. Biochem. Cytol.* 4:349–364.
- Rome, E. 1968. X-ray diffraction studies of the filament lattice of striated muscle in various bathing media. *J. Mol. Biol.* 37:331–344.
- Rumsby, M. G., and A. J. Crang. 1977. The myelin sheath—a structural examination. In *The Synthesis, Assembly and Turnover of Cell Surface Components*. Poste, G. and Nicolson, G. L., editors. pp. 247–362. Elsevier-North-Holland Biomedical Press, Amsterdam.
- Rushton, W. A. H. 1951. A theory of the effects of fibre size in medullated nerve. *J. Physiol. Lond.* 115:101–122.
- Schmitt, F. O., R. S. Bear, and G. L. Clark. 1935. X-ray diffraction studies on nerve. *Radiology* 25:131–151.
- Schulz, G. E., and R. H. Schirmer. 1979. Principles of Protein Structure. Springer-Verlag, New York, Inc.
- Sculley, M. J., J. T. Duniec, S. W. Thorne, W. S. Chow, and N. K. Boardman. 1980. The stacking of chloroplast thylakoids: quantitative analysis of the balance of forces between thylakoid membranes of chloroplasts, and the role of divalent cations. *Arch. Biochem. Biophys.* 201:339–346.
- Sornette, D., and N. Ostrowsky. 1986. Importance of membrane fluidity on bilayer interactions. *J. Chem. Phys.* 84:4062–4067.
- Stoffel, W., H. Giersiefen, H. Hillen, W. Schroeder, and B. Tunggal. 1985. Amino-acid sequence of human and bovine brain myelin proteolipid protein (Lipophilin) is completely conserved. *Biol. Chem. Hoppe-Seyler* 366:627–635.
- Tasaki, I. 1955. New measurements of the capacity and the resistance of the myelin sheath and the nodal membrane of the isolated frog nerve fiber. *Am. J. Physiol.* 181:639–650.
- Verwey, E. J. W., and J. Th. G. Overbeek. 1948. Theory of the Stability of Lyophobic Colloids. Elsevier, North-Holland, Inc., New York.
- Worthington, C. R. 1979. An x-ray study of the pH property of frog sciatic nerve. *Int. J. Biol. Macromol.* 1:157–164.
- Worthington, C. R. 1982. The physical states of nerve myelin. In *Membranes and Transport, Volume 2*. Martonosi, A. N., editor. pp. 389–394. Plenum Publishing Co., New York.
- Worthington, C. R., and A. E. Blaurock. 1969. A low-angle x-ray diffraction study of the swelling behavior of peripheral nerve myelin. *Biochim. Biophys. Acta* 173:427–435.
- Worthington, C. R., and A. R. Worthington. 1981. Effect of heat on frog sciatic nerve determined by x-ray diffraction. *Int. J. Biol. Macromol.* 3:159–164.